Integrity Monitoring of Adhesively Bonded Joints via an Electromechanical Impedance-based Approach

Yitao Zhuang[1], Fotis Kopsaftopoulos[2*], Roberto Dugnani[3], Fu-Kuo Chang[1]
[1]Department of Aeronautics and Astronautics, Stanford University, Stanford, CA, 94305
[2]Department of Mechanical, Aerospace and Nuclear Engineering, Rensselaer Polytechnic Institute, NY, USA
[3]UM-SJTU Joint Institute (JI), 800 Dongchuan Rd, Shanghai, China

ABSTRACT

Monitoring the bondline integrity of adhesively bonded joints consists one of the most critical concerns in the design of aircraft structures up to date. Due to the lack of confidence on the integrity of the bondline both during fabrication and service, the industry standards and regulations require assembling the primary airframe structure using the inefficient "black-aluminum" approach, i.e. drill holes and use fasteners. Furthermore, state-of-the-art non-destructive evaluation (NDE) and structural health monitoring (SHM) approaches are not yet able to provide mature solutions on the issue of bondline integrity monitoring. Therefore, the objective of this work is the introduction and feasibility investigation of a novel bondline integrity monitoring method that is based on the use of piezoelectric sensors embedded inside adhesively bonded joints in order to provide an early detection of bondline degradation. The proposed approach incorporates: (i) micro-sensors embedded inside the adhesive layer leaving a minimal footprint on the material, (ii) numerical and analytical modeling of the electromechanical impedance (EMI) of the adhesive bondline, and (iii) EMI-based diagnostic algorithms for monitoring and assessing the bondline integrity. The experimental validation and assessment of the proposed approach is achieved via the design and fabrication of prototype adhesively bonded lap joints with embedded piezoelectric sensors and a series of mechanical tests under various static and dynamic (fatigue) loading conditions. The obtained results demonstrate the potential of the proposed approach in providing increased confidence on the use of adhesively bonded joints for aerospace structures.

INTRODUCTION

In the last decade, significant progress has been made in the development and improvement of methods for the investigation of adhesively bonded joints and structures. Bondline integrity monitoring is still one of the most critical concerns in the design of aircraft and spacecraft structures up to date. Although adhesively bonded joints have demonstrated superior properties over mechanically fastened joints, current standards still require the use of fasteners along with the adhesive due to the lack of confidence on monitoring the integrity of bondlines during both the fabrication process and service life. Regardless of the nature of adhesive and adherents, any adhesively bonded system may be considered as a multilayered assembly, in which the adhesive must provide the integrity of the whole construction. Therefore, potential structural defects of the

---

[*]Corresponding Author: Fotis Kopsaftopoulos, Department of Mechanical, Aerospace and Nuclear Engineering, Rensselaer Polytechnic Institute, Troy, NY, USA. Email: kopsaf@rpi.edu

Structural Health Monitoring, in press, 2017
https://doi.org/10.1177/1475921717732331

adhesive can negatively influence the integrity of the bonded joint and decrease the expected strength of the assembly [1-3].

The main bondline defects that can impact the quality of the adhesive strength are voids, discontinuities, delaminations, "kissing" bonds, porosity, air bubbles resulting from improper curing, variations in glue-line thickness, microcracks and microfractures. Such bondline and adhesive defects can appear during the fabrication of initial constituents, assembly of bond joints, and during the entire process of the assembly operation. Classification of defect types may be found in the wide surveys of Adams and Drinkwater [4] and Munns and Georgiou [5]. Defects may be classified into two main types according to their location: defects in the bulk of the adhesive layer and defects on the adhesive-substrate interface [1]. Defects in the bulk of the adhesive cause a decrease of cohesive strength and therefore a degradation of the bonded joint. Defects on the adhesive-substrate interface relate to the bonding process reducing the overall adhesive strength.

Several non-destructive evaluation (NDE) methods, such as visual inspection, optical and electron microscopy, X-rays, C-Scan, IR-thermography, and IR-radiometry, are available for bondline integrity evaluation [1-7]. Those methods have been proven to be effective to a certain extent, however they require time consuming special preparation of samples and therefore they cannot be used for serial examination on the same sample, or performed on large finished assemblies. In addition, the have limited potential for in-situ continuous and automated monitoring. Furthermore, IR and X-ray methods have no direct relation to the mechanical nature of the material, while the potential of the latter is limited to the evaluation of assemblies containing surface metallic layers.

On the other hand, acousto-ultrasonic wave methods, such as pulse-echo and transmission techniques, ultrasound spectroscopy, and guided-wave-based methods allow the collection of insightful information regarding the actual structure and material properties [6-20]. Moreover, these methods are sensitive to the mechanical properties of the adhesive and to the boundary conditions between the adhesive and the substrate. In this respect, they constitute irreplaceable tools for NDE of adhesively bonded joints and structures within the aerospace community. Towards this end, recent work in structural health monitoring (SHM), by Ihn and Chang [21-23], has demonstrated the ability to identify debonds in real-time using built-in piezoelectric discs to generate ultrasonic waves, however they cannot effectively tackle the early detection of weak adhesive bonds [21-23].

Apart from the acousto-ultrasonic methods, electromechanical impedance (EMI) based SHM techniques form an important family of methods that have shown promising results in monitoring structural integrity [24-31]. The basic concept of the EMI-based approach is to monitor variations in the EMI response caused by the presence of defects and/or damage. Oftentimes, these methods utilize active piezoelectric transducers, either bonded on the surface or embedded inside the host structure, that are used to directly measure the local dynamic response. By employing high-frequency ranges (>30 kHz), the such methods are very sensitive to localized incipient changes of the structural integrity.

It has been reported that there exists a type of adhesive defects corresponding to traction-free in-contact surfaces, which show reduced bonding strength and are difficult –or even impossible– to

detect using conventional NDE techniques [7-10]. The so-called "kissing" bonds are one of the major adhesive defects and possess little residual tensile or shear strength. Many factors may lead to kissing bonds, including amongst others surface contaminates, adhesive chemistry, inappropriate curing stresses, residual stresses, moisture ingress, etc. As a result, kissing bonds can appear in a local fashion and the only way to detect them is to measure the local adhesive during fabrication and in-service to track its degradation [6-10]. Kissing bonds are the most critical and challenging defect to be detected in adhesively bonded joints and significantly influence the confidence to bondline integrity after the joints are placed in service. In addition, they are extremely difficult to detect by acoustic and ultrasonic methods because the substrate may be in intimate contact with the adhesive layer, but without any adhesive bonding existing between the adhesive and the adherent. Current NDE techniques have demonstrated limited effectiveness in detecting early stage kissing bonds and by extension, ensure the quality of adhesive bonds [7-10]. In addition, they require the use of bulky equipment and well-controlled environment, thus face difficulties when it comes to the in-situ periodic or continuous monitoring of the bondline integrity.

Embedding micro/nano sensors inside the adhesive layer has the potential to be an effective solution to this challenge. Upon initial inspection, this approach may not seem feasible because adding new materials inside adhesive will increase the risk of contamination and introduce new defects. However, industry has begun to use adhesive films with fiber scrims inside, to ease handling and improve quality control. For example, Henkel embeds nylon scrim material into Hysol EA 9696 film adhesives. This indicates that shrinking the sensors down to the size of typical fibers and fabricating them from the same –or compatible– materials as current scrims may be a promising and feasible approach for that merits further investigation. Therefore, the adhesive will exhibit the same mechanical performance but at the same time will possess the capability to monitor its own integrity. To the authors' best of knowledge, there have been no previous studies that investigate the use of embedded active sensors directly into adhesive bondlines for integrity monitoring.

In recent studies [32-34], the authors and co-workers addressed the problem of bondline integrity monitoring via the use of piezoelectric transducers embedded inside adhesively bonded lap joints and monitoring the EMI signatures. The problem was tackled via an EMI-based cross-correlation approach [32] and a preliminary approach based on the use of EMI-based damage indices [33-34]. In these studies, the changes in the EMI with respect to static loading conditions showed significant potential in successfully diagnosing the degradation of the bondline. Therefore, the present study aims at the postulation and extended experimental assessment and evaluation of an EMI-based method for monitoring the integrity of adhesively bonded structures.

PROBLEM STATEMENT

Monitoring the integrity of adhesively bonded structures, based on both composites and metallic materials, is an extremely challenging task and no mature solutions have been yet proposed in the state-of-the-art literature. Therefore, the objective of this work is the introduction and feasibility investigation of a bondline integrity monitoring approach that is based on the use of piezoelectric sensors embedded into adhesively bonded joints to provide an early detection of degradation.

Given piezoelectric transducers it is desired to: (i) develop a fabrication approach to embed them inside the adhesive scrim of shear lap joints, (ii) develop appropriate experimental procedures for

assessing the bondline integrity, and (iii) develop an appropriate diagnostic method for enabling the early detection of bondline degradation. The proposed approach is based on the use of piezoelectric micro-sensors embedded inside the adhesive layer leaving a minimal footprint on the material, numerical and analytical modeling of the EMI of the adhesive bondline, and EMI-based diagnostic algorithms for monitoring and assessing the bondline integrity.

EXPERIMENTATION

Characterization of Carbon Fiber Reinforced Panels with Simulated Kissing Bond

Static shear testing was conducted on a single shear sample fabricated by Boeing to understand the effect of kissing bonds on the bondline performance. The sample consisted of two carbon fiber reinforce plastic panels (152.4 mm x 457.2 mm or 6 inch x 18 inch) bonded together with Hysol EA9696 adhesive film. One panel consisted of a 16 plies (0-90 fabrics on the first and last layer, and $[-45/90/45/-45/0/45/0]_s$ in the middle) and the other of 20 plies (0-90 fabrics on the first and last layer, and $[-45/90/45/0/-45/0/0/45/0]_s$ in the middle). The thickness of the coupon is 7.24 mm and the bondline is approximately 0.4 mm thick. Using an in-house developed approach on surface preparation, Boeing could tune the bondline strength into different levels. On the samples provided by Boeing, three levels of strength were achieved on different regions and were characterized as weak (strength predicted to be 8.62 MPa or 1250 psi), medium (17.24 MPa or 2500 psi), and nominal (27.58 MPa or 4000 psi) bond. The bonded panels were cut into 25.4 mm x 152.7 mm (1 inch x 6 inch) strips with the notch of 2.54 mm (0.1 inch) width following ASTM D5868 (Standard Test Method for Lap Shear Adhesion for Fiber Reinforced Plastic (FRP) Bonding) in order to evaluate the bondline strength in static shear load test. The loading was measured by the load cell of the Material Testing System (MTS) and the displacement was measured directly by the internal extensometer.

The load-displacement test results and the failure patterns are shown in Figure 1. The bondline area was 650 mm^2 and the shear stress was estimated by dividing the load by the area directly. The strength of the weak bond was measured at 13.58±7 % MPa (1970±7 % psi), the medium bond at 20.89±2 % MPa (3030±2 % psi) and the nominal bond at 28.68±4 % MPa (4160±4 % psi). The failure patterns of weak and medium bonds indicated adhesive failure, while the pattern of the nominal bond indicated a cohesive failure. The kissing bond (weak) resulted in a 50 % loss of strength compared to the nominal bond and the failure pattern indicated that the weak adhesion between adhesive and substrate material caused the decrease of the bondline strength. The load-displacement curves of different strength levels overlapped, which demonstrates that the existence of kissing bonds has a very limited effect on the global stiffness of the bonded structure.

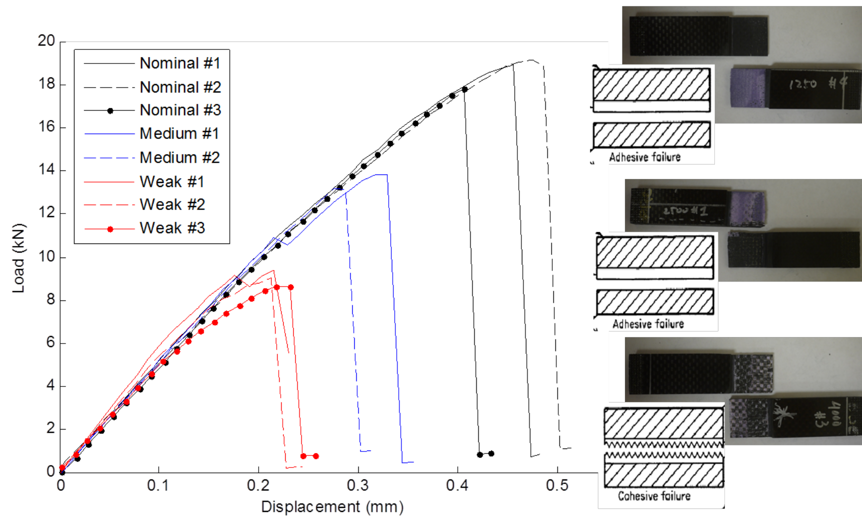

Figure 1. The load-displacement characteristic of bonded joints with three levels of bondline strength and the corresponding failure patterns (top: weak; middle: medium; bottom: nominal).

Adhesively Bonded Aluminum Single Lap-Shear Coupons

This section outlines the development of a process to prepare the adhesively bonded aluminum single lap-shear coupons with commercially available PZT sensors (1/8 inch diameter) embedded in the bondline. After their fabrication, the coupons were loaded under static loading to study the response of the embedded sensors. Single lap joints with embedded PZT sensors were prepared to investigate the relationship between the electromechanical impedance behavior of the sensors and the load history of the lap joints (see Figure 2 and Figure 3). The samples were prepared following the ASTM D1002 (Standard Test Method for Apparent Shear Strength of Single-Lap joint Adhesively Bonded Metal Specimens by Tension Loading (Metal-to-Metal)), with 25.4 mm by 25.4 mm (1 inch by 1 inch) of bondline area for one sensor embedded.

Hysol EA 9696 adhesive film provided by Henkel was used to bond two aluminum alloy laps (2024 T5). Hysol EA 9696 is a modified epoxy film designed for applications requiring high toughness including aeronautics. The adhesive of this study was provided by Boeing. The adhesive films were sealed and stored in -18 °C in the Structures and Composites Laboratory at Stanford University**.** The surface preparation procedure is designed to follow the ASTM standard D2651, Standard Guide for Preparation of Metal Surfaces for Adhesive Bonding. The preparation steps are the following**:**

- De-ionized water rinse
- Abrade surfaces with sandpaper (3M Medium 100 Grit)
- Compressed air blow
- De-ionized water rinse
- Isopropyl alcohol rinse, rubbed with cotton
- De-ionized water rinse
- Acetone rinse, rubbed with cotton
- De-ionized water rinse
- Dried in 60 °C oven

In order to simulate the "kissing" bond behavior, four types of chemicals were used to degrade the bondline strength, namely silicone, teflone, graphite powder and polydimethylsiloxane (PDMS). All four contaminates were applied to the interface of different samples before curing. Next, the samples were loaded to measure the loss of the shear strength. PDMS led to 97% loss of the strength; graphite powder led to 77% loss of strength; Teflon led to 63% loss, and silicone led to only 10% loss of strength. Graphite powder was used as the surface contaminate in the latter tests due to its large influence on the bond strength and relative ease to handle.

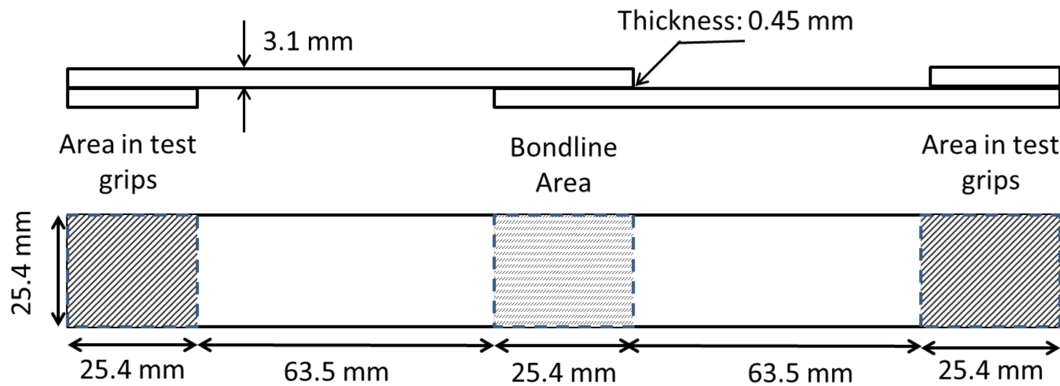

Figure 2. Design and dimensions of single lap joint test specimen for apparent shear strength, adapted from the standard ASTM D1002.

Piezoelectric disc sensors fabricated by APC ceramics were embedded inside the bondline. The piezo material was Navy II type equivalent with 250 um in thickness and 3.1 mm (1/8 inch) in diameter. The material properties can be found in Table 1; the out-of-plane direction was defined as the third direction.

Table 1. The properties of the piezoelectric material in APC disc sensor (Material: PZT-5A).

Density	Young's Modulus E_{11}	Young's Modulus E_{33}	Relative Dielectric Constant K_T	Piezo Charge Constant d_{33}	Piezo Voltage Constant g_{33}
7.6 g/cm^3	63 GPa	54 GPa	1900	400 pC/N	24.8 mV-m/N

Due to the thickness of the piezoelectric disc sensors, three to four layers of adhesive film were used to fully encapsulate the sensors. Two varnished wires (AWG 40) with diameter of 80 um were also embedded to extend the two electrodes of the sensor to the outside of the bondline, which were subsequently connected to a PC-connected impedance analyzer (Model 16777K SinePhase Instruments). The lay-up of the sample is illustrated in Figure 3. Following the instruction of the manufacturer, the samples were cured under vacuum for 90 minutes at 121 °C.

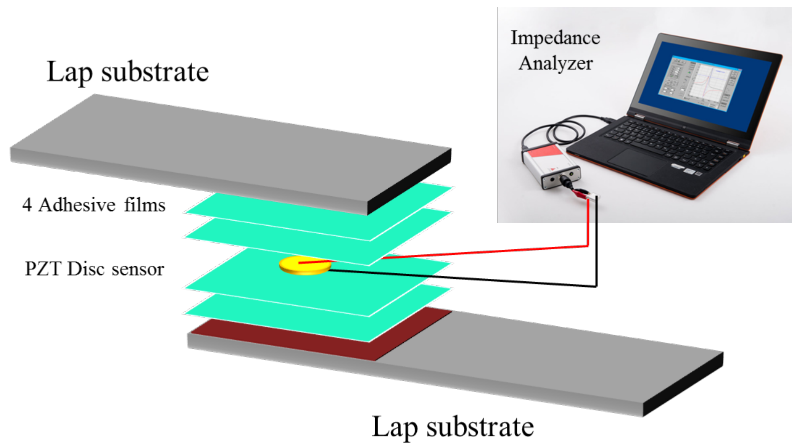

Figure 3. Illustration of a single lap joint with one piezoelectric sensor embedded into the adhesive bondline interface.

The fabricated samples were loaded on the MTS so that the introduced static loads could further degrade the bondline integrity and allow the appearance of the kissing bond. The overall setup is shown in Figure 4. The implemented load had was increased by a step of 111 N (25 lbs). After the static loading of the lap joint the shear load was decreased to zero and the electromechanical impedance was measured under zero-loading condition by the impedance analyzer. Next, the lap joint was subjected to a higher load based on the specified increment and subsequently unloaded again for data collection. This process continued until the failure of the lap joint. A typical load history curve is illustrated in Figure 5. The impedance behavior of the piezo was recorded in the range of 1 KHz to 2.5 MHz with an increment of 1 KHz. Both the real and imaginary impedance data were acquired. The cyclic load with an incremental peak value was exerted on the specimens.

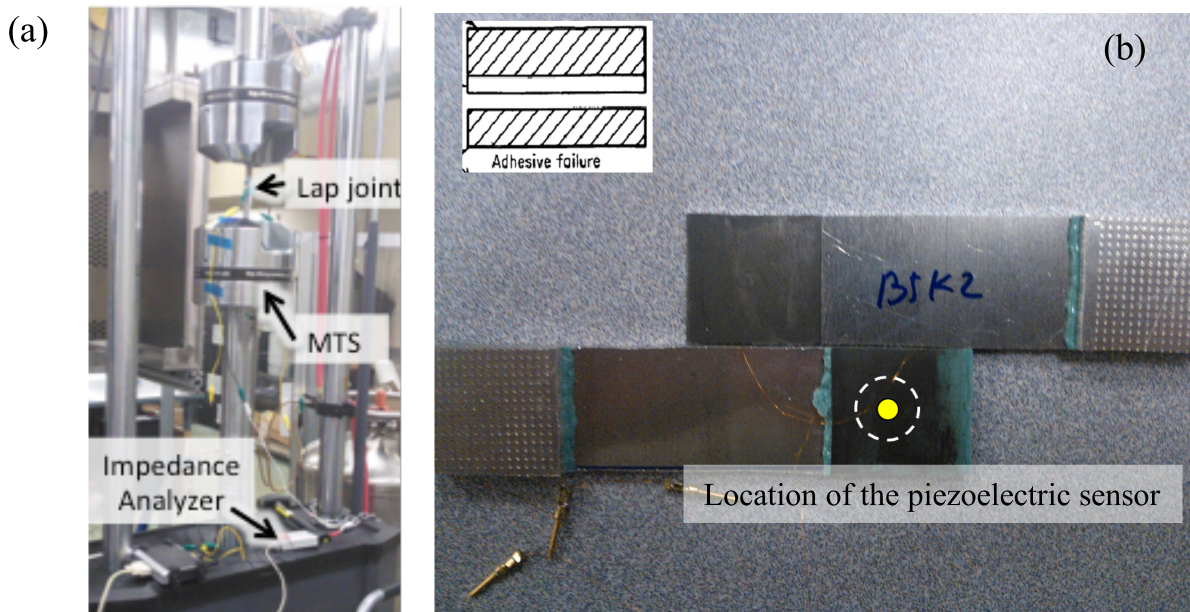

Figure 4: (a) The experimental test setup; (b) the sample with the embedded sensor exhibited an adhesive failure mode due to the surface contamination with graphite powder.

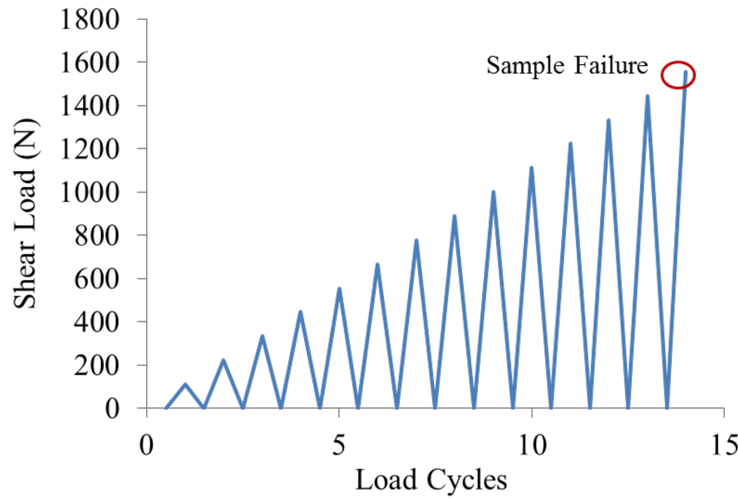

Figure 5. Typical shear load cycle with the impedance measured under the unloaded condition (zero shear load) in order to minimize the loading effect on the piezoelectric sensor.

RESULTS

Impedance Behavior of Embedded Piezoelectric Sensors after Static Loading

A typical EMI behavior of the samples is presented in Figure 6. There are two resonant peaks shown in the measured frequency bandwidth between 500 KHz and 2.5 MHz. The first peak is recorded around 800 KHz and the second peak with a lower amplitude is found around 1.7 MHz. The two EMI resonate peaks are related to the radial and thickness vibration modes, respectively. A similar impedance behavior was observed throughout all the samples under all loading conditions with slight differences in the frequency and amplitude.

Several damage indices that appear in the literature were investigated in order to evaluate the influence of the load cycles on the behavior of the piezoelectric sensors and the bondline integrity. The Root Mean Square Deviation (RSMD) was selected as an appropriate damage index (the differences with other commonly used EMI-based damage indices were minor), which describes the average impedance change from the baseline sample without any loading. The definition of RMSD is shown in Equation (1), where $Z_h(\omega_i)$ is the healthy bond's impedance, $Z_u(\omega_i)$ is the unknown or damaged bond's impedance and ω_i is the frequency interval.

$$\text{Damage Index} = \sqrt{\frac{\sum_{i=1}^{n}[Re(Z_h(\omega_i)) - Re(Z_u(\omega_i))]^2}{\sum_{i=1}^{n}[Re(Z_h(\omega_i))]^2}} \qquad (1)$$

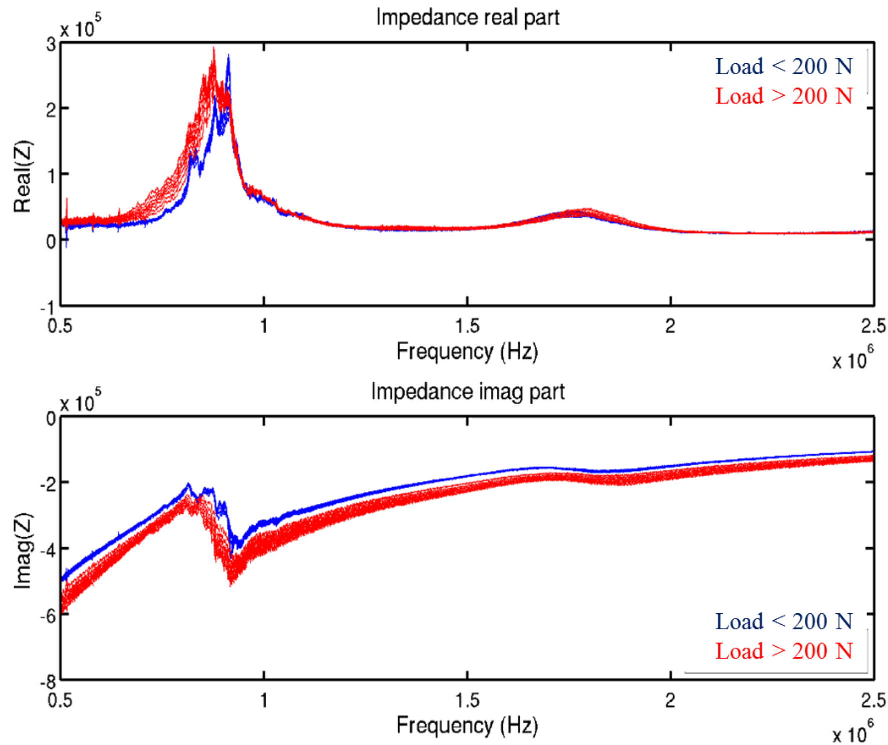

Figure 6. Typical EMI behaviour obtained from experimental samples under different loads.

The damage index was estimated via the use of the EMI data centered in the first peak frequency and within a range of 100 kHz. Regardless of the existence of surface contaminates, all samples showed a similar behavior, i.e. the damage index was relatively constant until the sample was exposed to a certain level of load cycle and approaching failure. This implies that by measuring the EMI and the deviation of impedance from the intrinsic sample, it is possible to predict the failure of the bonded joint and estimate the degradation of the bondline. For example, as shown in Figure 7, a value of 2% in the damage index was selected as an arbitrary threshold to characterize the bondline state either as healthy or degraded.

Since the strength of the bondline was different across different batches, the max stress in load cycles was normalized by the strength of the bondline. The results are shown in Figure 8. It is evident that all the curves show the similar trend, i.e. the damage index stays relatively constant regardless of the stress experienced up until around 80% ~ 90% of the failure stress. After this stress threshold, the damage index increases dramatically with the increase of the load, which implies that the failure is approaching. The curves of the green color showed a similar trend while the damage index ramped up after a much lower stress level. After the test, it was observed that the sensor was fractured, which had not been seen on other samples, and it indicated that the outliner was due to the premature failure of the embedded sensor.

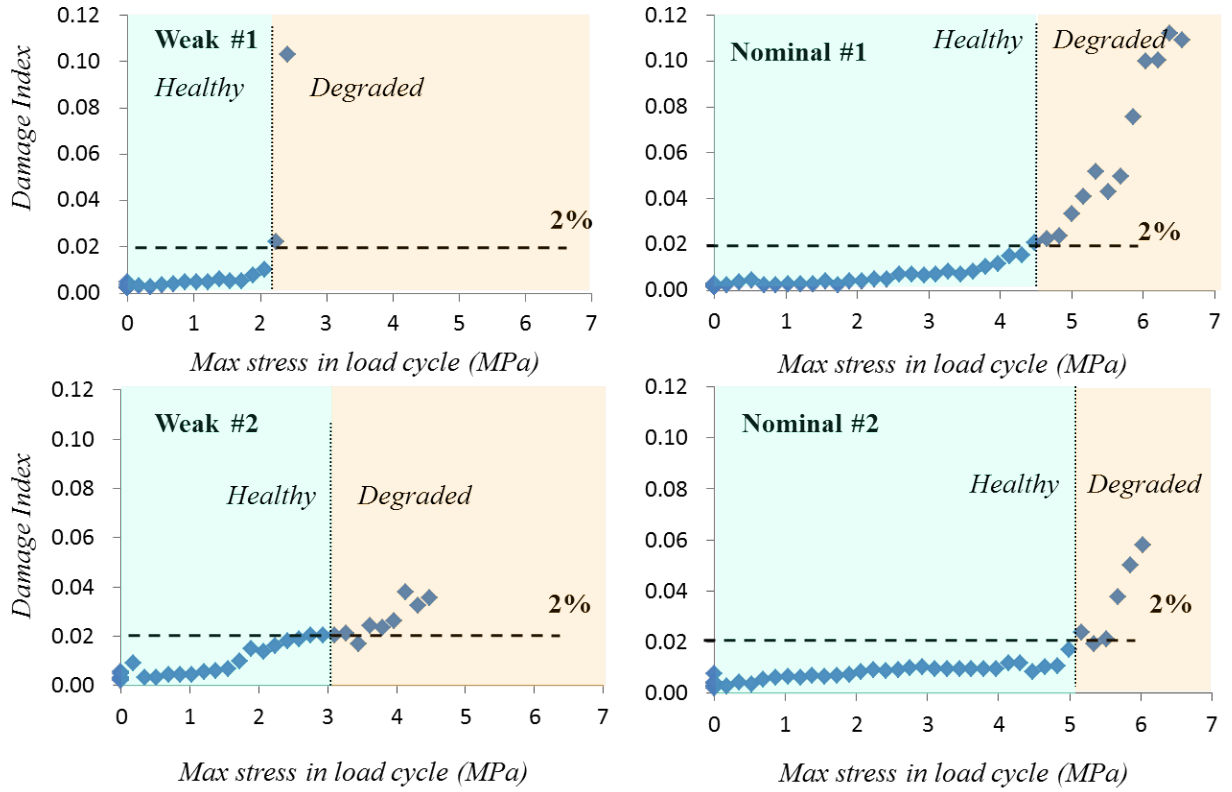

Figure 7. The damage index (Root Mean Square Deviation) of both weak and nominal samples exhibited a similar trend.

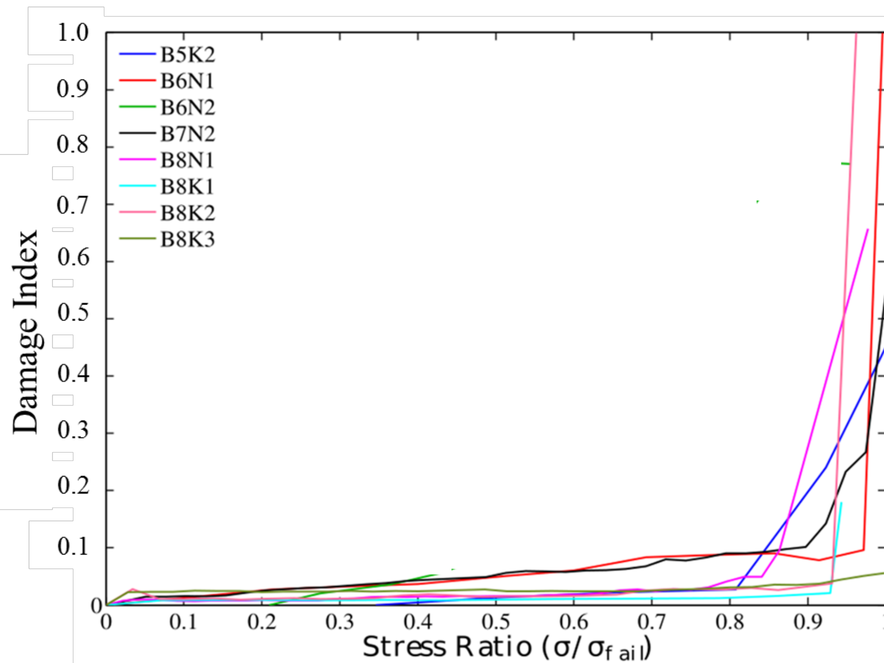

Figure 8. The damage index (root mean square deviation) of most samples exhibited a similar trend: a large increase of the damage index after approximately 80% of the lap joint strength.

Finite Element Simulation Study

A finite element model (FEM) has been developed using the commercial software Abaqus 6.12 to simulate the EMI behavior of the embedded sensors. The aim was to obtain a qualitative representative result of the impedance behavior over the large frequency bandwidth using the direct steady-state linear dynamic analysis. The overall dimension of the single lap joint is the same as the design described in Figure 2, yet the thickness of the bondline was adjusted to 0.55 mm to include a piezoelectric sensor with 0.25 mm thickness. The sensor is made from piezoelectric material PZT-5A and has a disc shape with diameter of 3.1 mm. C3D8E elements, that is solid elements with built-in piezoelectric properties, were used to model the piezoelectric material. The mesh of the sensor had a typical dimension of 100 um to capture all the motion and deformation of the sensor. The sensor was connected to the adhesive via a tie-connect. A convergence study was conducted and the simulation result converged at mesh size of 200 um. The impedance behavior from 50 KHz to 2 MHz was calculated at the interval of 5 KHz. For the highest frequency of 2 MHz, the typical wavelength of the mechanical wave in the adhesive would be on the order of mm, and the mesh was fine enough to capture it.

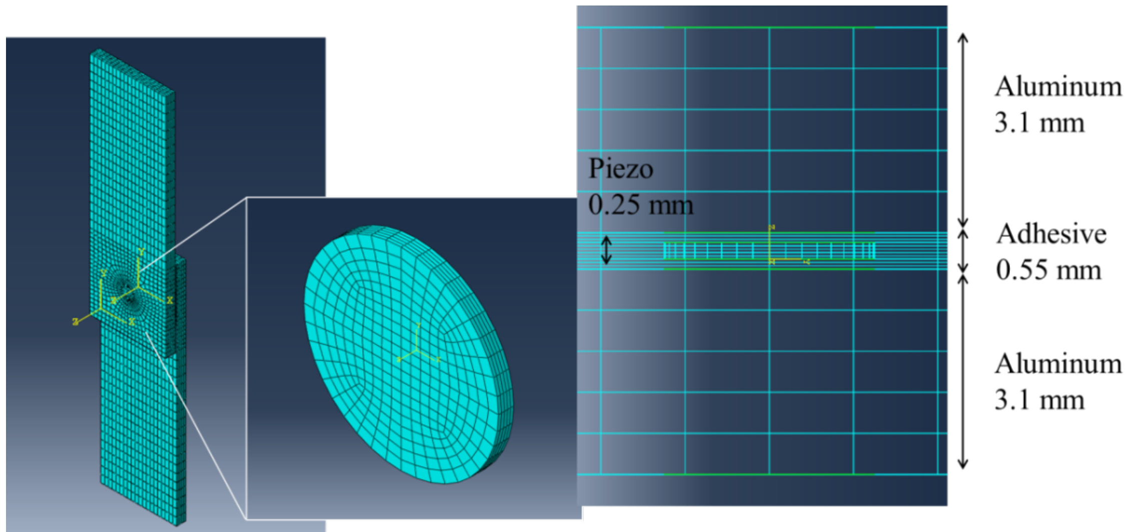

Figure 9. The FEM model and mesh of the bondline with embedded piezoelectric sensor disc.

The material properties used in the simulations are shown in Table 2 [35].

Table 2. Material properties (mechanical properties) used in the numerical simulations; the direct piezoelectric effect matrix [d] and permittivity [ε] of piezoelectric material are shown in matrices.

Property	Unit	Aluminum Al 2024-T3	Adhesive Hysol EA 9696	Piezo PZT-5A
E_{11}	GPa	69	2.6	60.97
E_{22}	GPa	69	2.6	60.97
E_{33}	GPa	69	2.6	53.19
G_{23}	GPa	25.94	1	21.05
G_{31}	GPa	25.94	1	21.05
G_{12}	GPa	25.94	1	22.57
ν_{23}		0.33	0.3	0.4402
ν_{13}		0.33	0.3	0.4402
ν_{12}		0.33	0.3	0.3500
ρ	kg m^{-3}	2700	1100	7750

$$d = \begin{bmatrix} 0 & 0 & 0 & 0 & 584 & 0 \\ 0 & 0 & 0 & 584 & 0 & 0 \\ -171 & -171 & 374 & 0 & 0 & 0 \end{bmatrix} \times 10^{-12} CN^{-1} \qquad \varepsilon_\sigma = \begin{bmatrix} 1730 & 0 & 0 \\ 0 & 1730 & 0 \\ 0 & 0 & 1700 \end{bmatrix} \times \varepsilon_0$$

In order to simulate the kissing bond behavior, a thin adhesive layer at the interface of the adherent and adhesive was modified (see Figure 10). The stiffness of that thin layer was decreased by changing the modulus of the adhesive material homogeneously across the whole bondline area. A similar method was mentioned in previous studies [2,3]. The typical thickness of the elements is 10 um as shown in Figure 10. The stiffness of the interfacial element is tuned to different levels (from 10% up to 90% of the original stiffness) to simulate different levels of severity of the bondline degradation due to kissing bond.

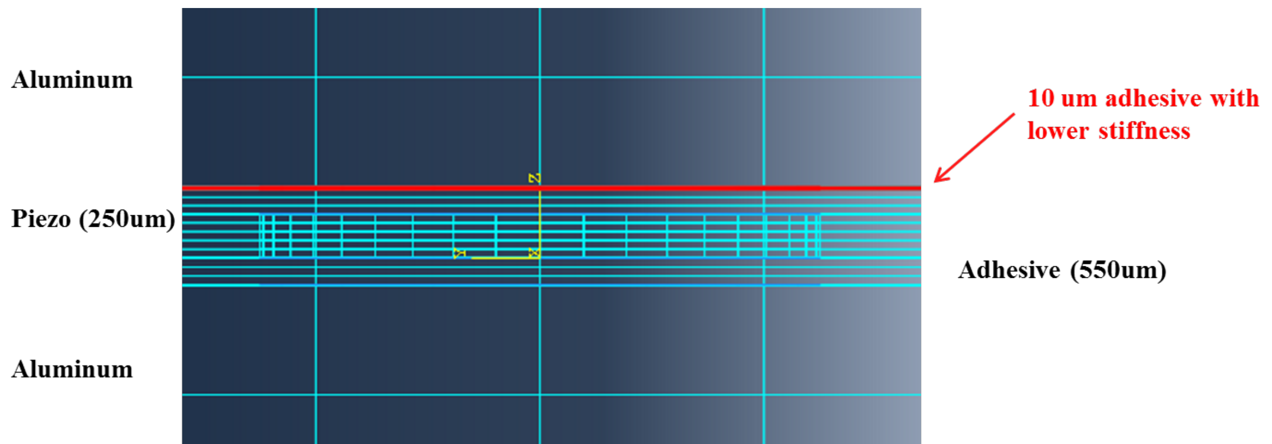

Figure 10. Kissing bond simulation is achieved via the reduction of the stiffness of the interfacial elements.

A direct steady-state dynamic analysis was performed to calculate the total electrical charge generated at each give frequency. The impedance of the piezo sensor was then calculated based on the electric charge, which is in the complex form. The simulation results for both the real and

imaginary parts are illustrated in Figure 11. The corresponding experimental results are also shown in solid line. The simulation results showed a good agreement with the corresponding experimental in both frequency and amplitude. The simulation result was sensitive to the stiffness or the modulus of the adhesive material as well as the damping coefficient of the piezoelectric sensor and the adhesive, which are difficult to accurately measure experimentally. With better calibration of the material properties, the simulation results could have shown a better match with the experimental result. However, the goal of the FEM analysis was to provide an understanding and qualitative insight on the bondline degradation mechanism.

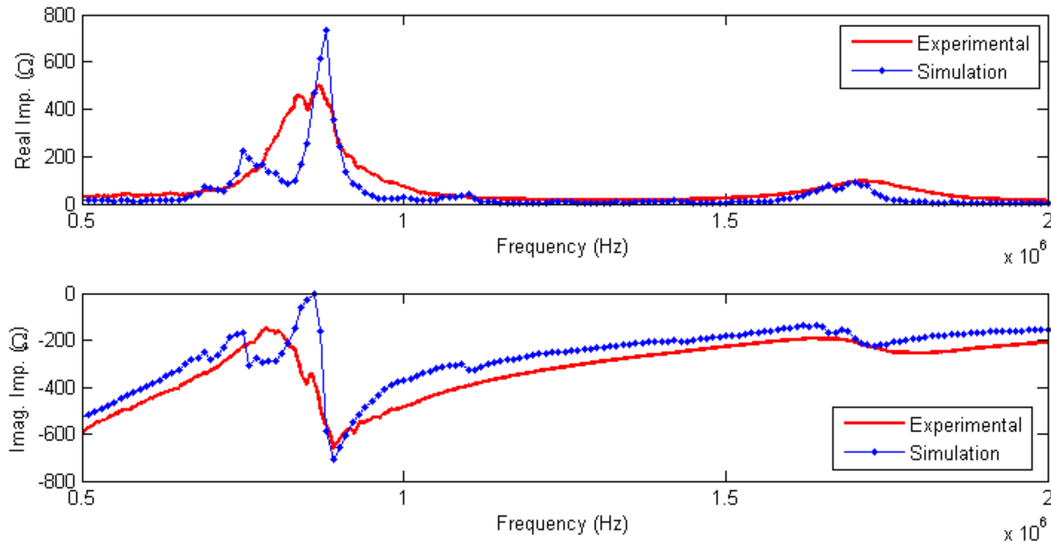

Figure 11. Comparison of numerically simulated and experimentally obtained impedance behaviour for a piezoelectric sensor embedded in the adhesive bondline.

The effects of decreasing the interfacial elements' stiffness on global stiffness of the structure were also studied. An 8750 N (1967 lbs) force was applied on one end of the single lap while the other end was fixed. The resultant displacement was 0.163 mm (6.4 x 10^{-3} inch) for the model when no decrease in the stiffness of the interfacial elements occurred, and 0.165 mm (6.5 x 10^{-3} inch) for the model whose interfacial elements' stiffness was decreased to 10% of the original stiffness. The decrease of interfacial elements' stiffness by 90% led to 1.4% increase of the end displacement. In conclusion, it may be assessed that the global stiffness of the lap joint is insensitive to the interfacial element stiffness, which was also confirmed by the experiments shown in Figure 1.

The stiffness was lowered from 10% up to 90% and the results of the simulation are plotted in Figure 12. With the decrease of the stiffness, the peak of the impedance initially decreases in the amplitude. After a certain level, the peak amplitude starts to increase while the frequency of the peak decreases. A similar trend was also observed experimentally when the load level of the sample increased and the damage level of the bondline became more severe as shown in Figure 13.

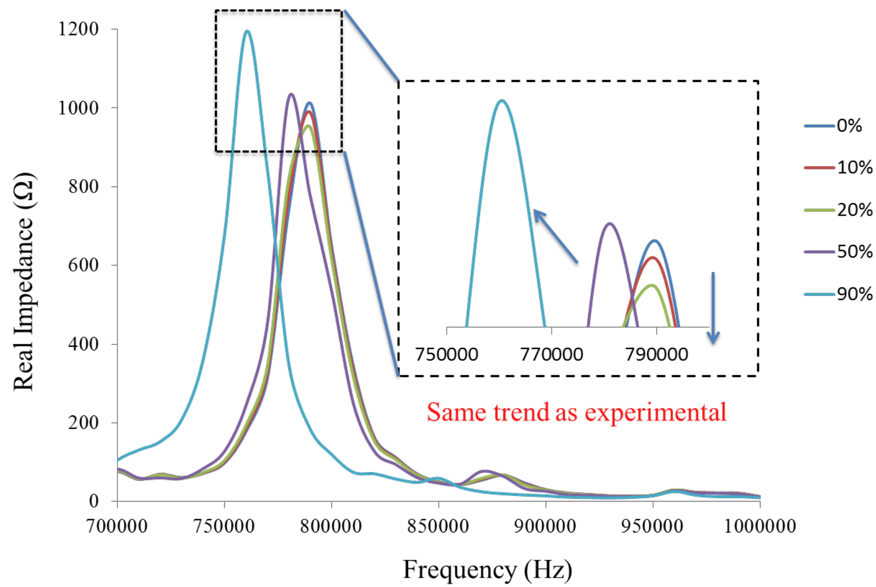

Figure 12. Numerical results for the simulation of the bondline integrity degradation due to kissing bond. The impedance peak initially decreases at a low level of bondline degradation (up to 20% loss of stiffness of the interface) and shift towards the lower frequency region when the level degradation is higher (more than 50% loss of stiffness of the interface).

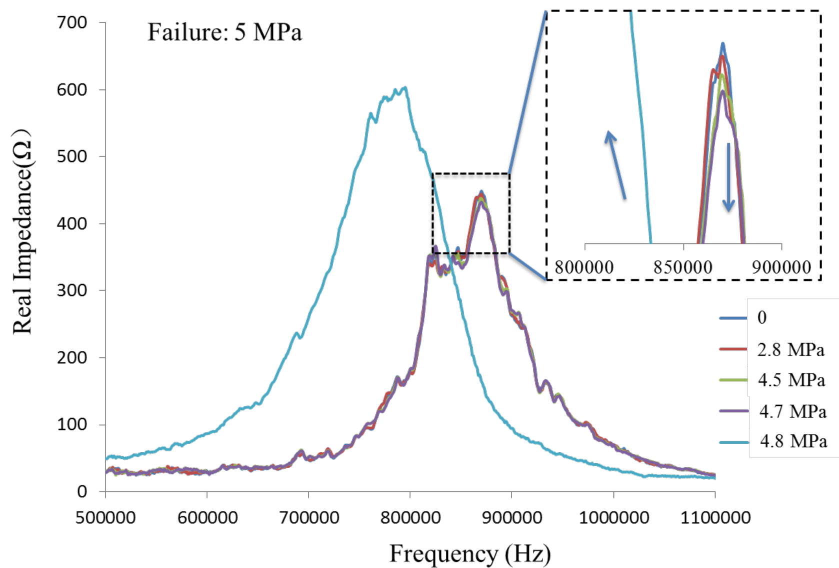

Figure 13. Experimental results of the impedance show a similar trend as the simulation results of Figure 12. After the sample was exposed to low level of shear stress (< 4.7 MPa), the amplitude of the impedance peak decreased; after the sample was exposed to high level of shear stress (>4.8 MPa), the impedance peak would shift to the lower frequency region.

DISCUSSION

Parasitic Effect of the Embedded Sensor on Mechanical Performance of the Adhesive Joints

By embedding sensors into bondlines, it is possible that the induced parasitic effect could degrade the mechanical performance of the bonded joints. In order to verify the influence of the sensors, for each batch manufactured, two extra lap joint samples without embedded sensors were prepared to compare the strength of the joints with the joints with sensors. As shown in Table 3, the effect of the embedded sensor has a very small impact on the strength of the lap joints when mounted in the middle point of the bondline.

Table 3. Lap joint strength with and without embedded sensors (sensor diameter: 3.1 mm); the difference is insignificant compared to the variation of measurements.

	Nominal Bond	Weak Bond
Strength (Lap without sensor)	22.1 ± 2.0 MPa	8.3 ± 4.3 MPa
Strength (Lap with sensor)	20.7 ± 1.2 MPa	9.3 ± 3.7 MPa

However, the thickness of the sensor is still one of the major concerns related to the sensor integration into the bondline. In practice, the optimal thickness of the bondline is between 0.2 mm to 0.5 mm, and any bondline thicker than 0.5 mm could lead to a less than optimal mechanical performance. As a result, it is necessary to design a sensor with minimum thickness in order to control the thickness of bondline at its desired range.

Effect of Sensor Location on EMI Behavior

The EMI method proposed in this paper leverages the sensitivity of the embedded piezoelectric sensors to the local structural integrity and corresponding response of the bondline. Consequently, the sensors are less sensitive to the defects or bondline property degradation occurring at remote to the sensor locations.

In order to investigate the relative sensitivity of the embedded sensor to the location of the defect and bondline degradation, three piezoelectric sensors were positioned inside a larger bondline (50.8 mm by 25.4 mm or 2 inch by 1 inch) of a single lap joint. As shown in Figure 14, two sensors were located in the middle and near the edge (6.4 mm or 0.25 inch) of the bondline (notice that the sensor on the left was not working due to a wire connectivity issue). The lap joint was then loaded under static loading and following the same procedure as described in the previous section. The EMI response of both sensors was recorded.

For the single lap joint, it is known that the shear stress is not uniform along the direction of the load. The stress on the edge of the bondlines is in general greater than the stress in the center. As a result, when the lap joint is exposed to an external load, damage is expected to be initiated near the edge and slowly propagate towards the center. The bondline failed at 7.86 MPa (1140 psi) and the damage index of the centered sensor increased dramatically after the sample was exposed to 96% of its strength while the damage index of the sensor on the edge changed at a significantly lower load level (78%). This indicates that it is possible to determine the location of piezoelectric sensors so as to predict the failure of the bondline at a much earlier stage (e.g. in areas where the stress is concentrated). This also implies that in order to have the capability to monitor a large area

of bondline, which is usually common in real-life applications, a large number of distributed sensors would be essential.

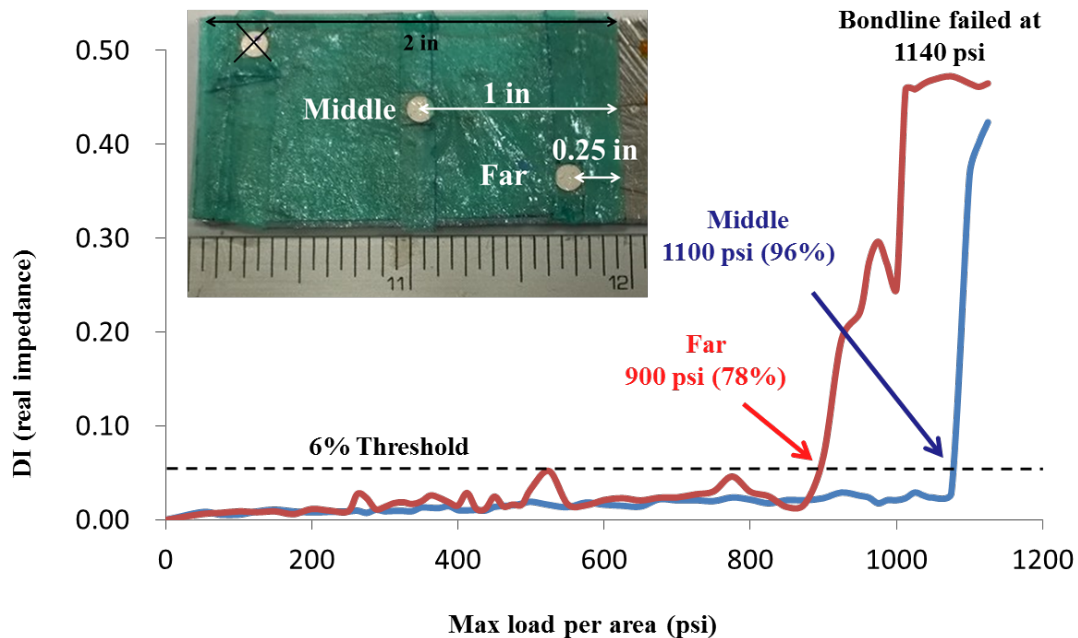

Figure 14. Indicative bondline degradation monitoring results with multiple piezoelectric sensors. The sensor on the edge is more sensitive to bondline degradation then the sensor on the edge.

Impedance Behavior of Embedded Piezoelectric Sensors after Fatigue Loading

A similar test under cyclic external loads was conducted in order to validate the EMI-based method under fatigue loads. The procedure for sample preparation and surface contamination was identical to the test under static loads, as described in the previous section. The batch was measured with a bondline thickness of 406 um (0.016 inch) with a variance of less than 25.4 um (0.001 inch). Graphite was used to contaminate the interface of adhesive and adherent. Three additional samples without sensors were fabricated in order to provide an estimated strength of the lap joints; the bondline strength was measured at 3.45 MPa [500 psi], i.e. 29% of the estimated nominal strength or 11.72 MPa [1700 psi]. The frequency of the fatigue loading was set to 3 Hz and the level of the load was set to the range of 0 and 2 MPa (300 psi). The EMI was recorded after certain number of load cycles and the sample was cyclically loaded until failure.

The EMI of the sample was recorded at the interval of 500 load cycles under zero-load condition. The EMI results are illustrated in Figure 15. There were two resonant peaks in the range of 300 KHz to 2.5 MHz. The first peak is located around 900 KHz while the second one around 1.8 MHz. The fatigue life was 48,000 cycles. Before 36,000 cycles (75% of full fatigue life), the EMI response of the embedded sensor almost overlaps, as shown in Figure 13. After 36,000 cycles, the EMI starts to deviate from its pristine state (Figure 15).

The RMSD between 800 KHz and 1 MHz was calculated and illustrated in Figure 16. Regardless of the impedance behavior after the initial fatigue load, the impedance was relatively constant until approximately 42,000 cycles (88% of the fatigue life). After that, the damage index increased

dramatically. This observation is similar to the test results under static loads. As a result, it may be concluded that the EMI response of embedded piezoelectric sensors and the corresponding damage index evolution can be used as an indicator of the failure of the adhesively bonded lap joint under fatigue/dynamic loading.

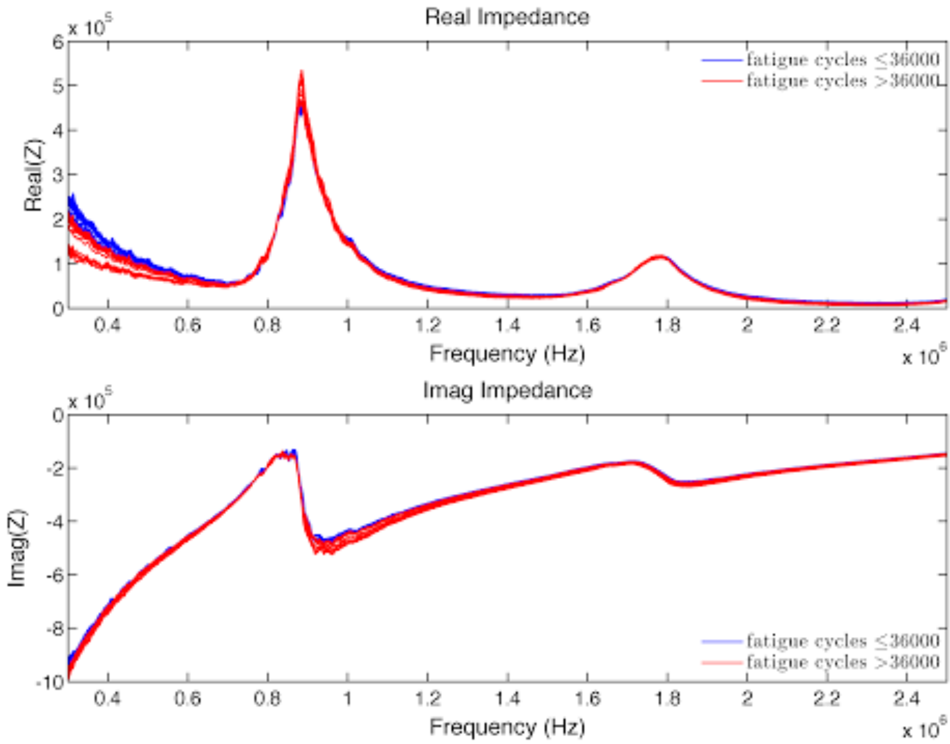

Figure 15. Real and imaginary parts of the electromechanical impedance of the embedded piezoelectric sensor in the adhesive bondline of the lap joint under fatigue loading.

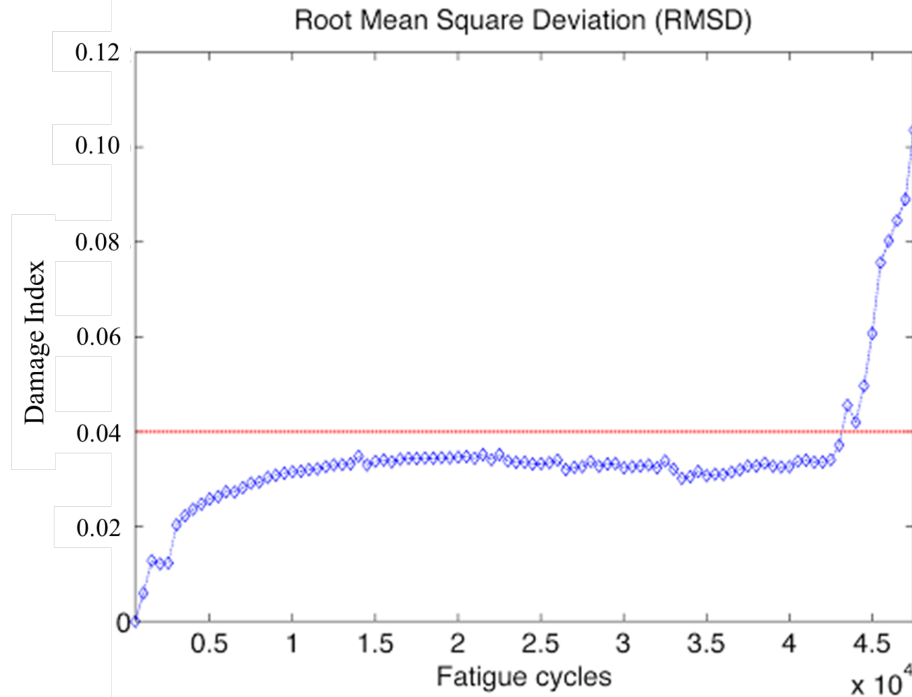

Figure 16. Damage index based on the root mean square deviation versus the number of fatigue cycles.

Parametric Study of Sensor Performance via Finite Element Simulations

In order to enable the successful implementation of the proposed method and achieve accurate monitoring results, the dimensions of the piezoelectric sensors have to be further reduced to achieve a minimal parasitic effect on the mechanical performance of the bonded joint. Meanwhile, the vertical position of the sensor, i.e. the distance of the sensor from the adhesive-adherent interface, can also affect the EMI response of the embedded sensor. Therefore, in this section a numerical investigation is conducted to assess potential sensor designs with respect to their sensitivity to bondline degradation.

There are three parameters studied to evaluate sensor's performance, i.e. the diameter and the thickness of the disc-shaped, centered, piezoelectric sensor embedded in the bondline as well as the distance to the degraded interface area, via a series of finite element simulations. As described in the previous section, the stiffness of the interfacial elements between adhesive and adherent were decreased for simulating bondline degradation. For each sensor design, three levels of stiffness degradation, nominal (0% of loss), degraded (10% of loss) and weak (50% of loss), were investigated. The EMI was simulated within the range of 50 kHz to 3 MHz under all the considered interfacial stiffness cases, and subsequently the damage index was calculated within the frequency range from 600 kHz to 3 MHz.

Initially, three sensor thicknesses, 250 um, 150 um and 50 um, were investigated. For each distinct case the diameter of the sensor was fixed at 3 mm and the distance to the bondline degradation was set to 150 um. The damage index based on the real impedance deviation is plotted in Figure 17. A monotonic relationship may be observed between the damage index and the thickness of the sensor under both degraded and weak levels of stiffness loss. The thinner the sensor, the higher

the damage index under the same level of bondline degradation. This implies that a thinner sensor design is preferred due to the better sensitivity to the degradation.

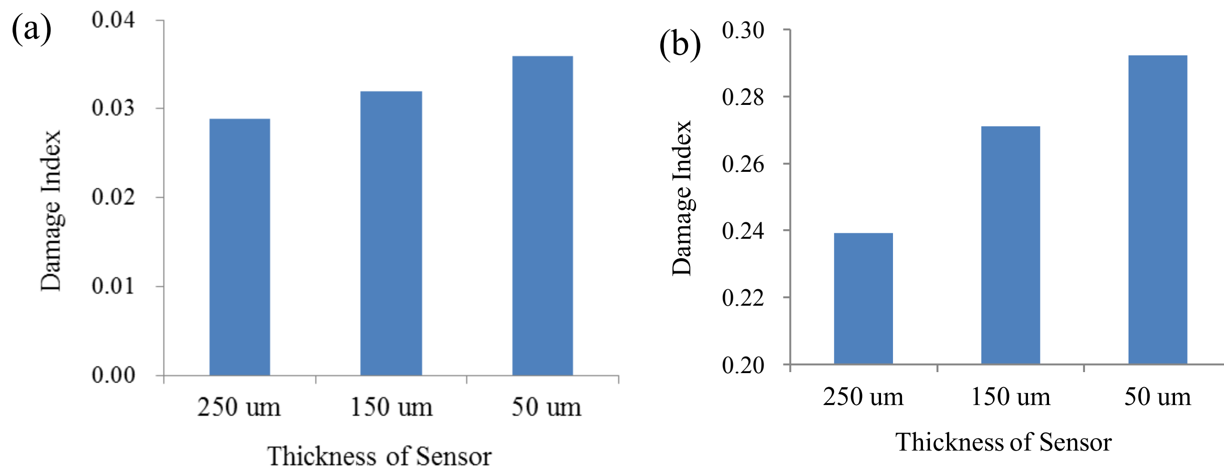

Figure 17. Shrinking down the thickness of the embedded sensor in the bondline leads to increased sensitivity regarding both the degraded bondline property (a: 10 % loss of interfacial stiffness) and weak bondline property (b: 50% loss of interfacial stiffness).

Three sensor diameters, 4 mm, 3 mm and 2 mm, were investigated while the thickness of the sensors was kept at 50 um and the distance to the bondline degradation was set to 150 um. The correlation is presented in Figure 18. Compared to the montonic dependence of thickness, shrinking down the diameter of sensors does not lead to a better performance. Instead, it seems that there is an optimal diameter for the embedded sensor to achieve a higher sensitivity with respect to the bondline degradation. In fact, based on the simulations, the 3 mm diameter design outperformed the 4 mm design by more than 100% for degraded case and more than 200% for the weak case.

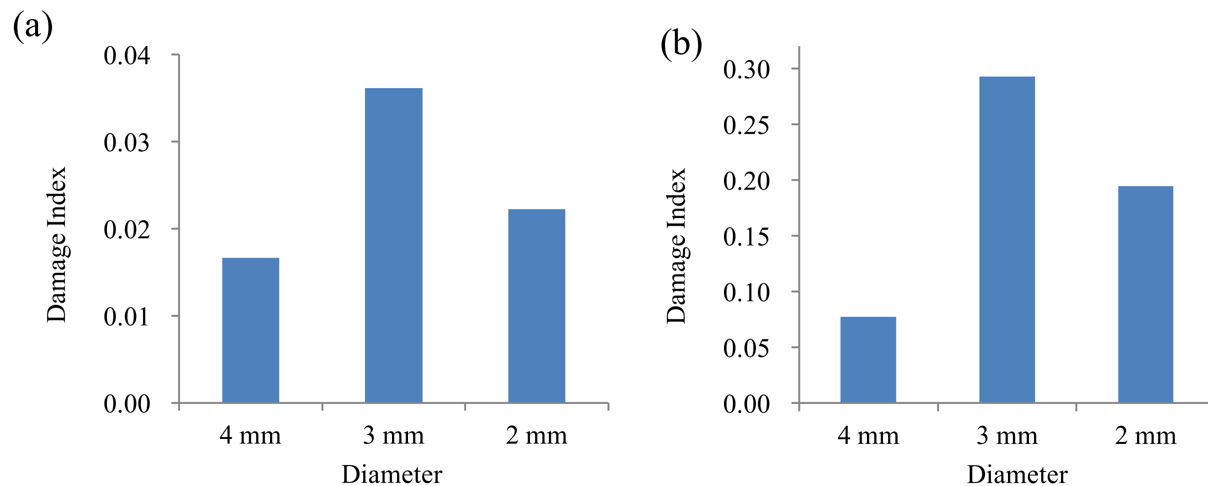

Figure 18. Shrinking down the diameter of the sensors led initially to increased sensitivity and subsequently to a slight decrease. A 3 mm sensor diameter achieved the highest sensitivity regarding both the degraded bondline property (a: 10% loss of interfacial stiffness) and weak bondline property (b: 50% loss of interfacial stiffness).

The last parameter investigated is the distance from the sensor to the interfacial element of which the stiffness was decreased to simulate bondline degradation. The bondline thickness was kept constant while the lateral distance was adjusted to study the sensor's performance. The sensor was designed with 2 mm diameter and 50 um in thickness while the thickness of the bondline was 350 um. The distance to the interface was set to 150 um, 100 um and 50 um, which meant that the sensor was placed from the midpoint to the nearer layer to the interface. The results are presented in Figure 19. There is no monotonic relationship between the distance and the sensor's sensitivity, which is realtively counter-intuitive. In fact, the sensitivity of the sensor was decreased when placed 100 um to the interface. This indicates that there is a complex interaction between the vibration on the sensor and the bondline structure. In order to find an optimal design, a thorough optimization process will be required to be investigated in a future study.

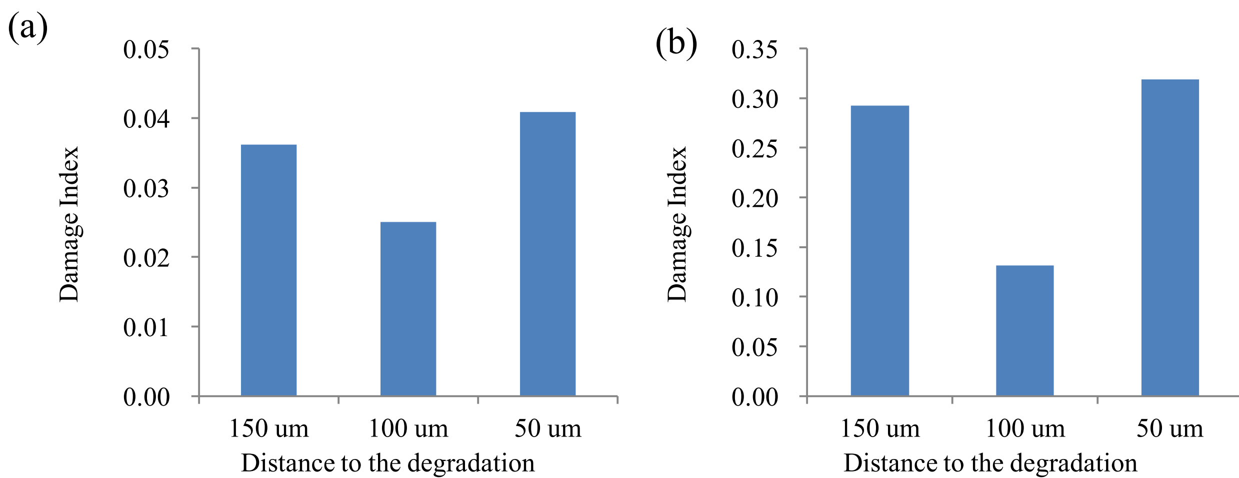

Figure 19. By placing the sensors closer to the bondline degradation, the sensitivity of the sensor was first decreased and subsequently increased. A 100 um distance results in the lowest sensitivity of the design of the sensor of 2 mm diameter and 50 um thickness to both the degraded bondline property (a: 10% loss of interfacial stiffness) and weak bondline property (b: 50% loss of interfacial stiffness).

CONCLUSIONS

Compared to conventional bolted joints, bonded joints have superior mechanical properties in terms of reduced weight, less stress concentration, and ease of fabrication. However, due to the lack of confidence on the bondline integrity during both fabrication and service, the large adaption of bonded joints onto airplane primary structural components is restricted by regulations and standards. Among all the defects that can be found in adhesive bondlines, one type of interfacial weakness, the kissing bond, is the most challenging one. This is due to the catastrophic failure it can cause to the bondline as well as to the almost impossible early detection using conventional non-destructive evaluation (NDE) or structural health monitoring (SHM) techniques. From the samples of bonded carbon-fiber reinforced plastic panels with simulated kissing bond fabricated by Boeing, a loss of more than 50% strength was observed without any significant change on global stiffness. In order to reproduce the kissing bond in our laboratory setting, several types of chemicals were tested to contaminate the interface between adhesive and adherent in the aluminum single lap joint. Graphite was chosen to reproduce kissing bond for the future study.

With the capability to simulate kissing bond behavior, we developed and tested a break-through technique to monitor the bondline integrity by embedding piezoelectric sensors into the bonded joints. The impedance-based detection algorithms were used by measuring the electromechanical impedance of the embedded sensors. Since the sensors are positioned in the bondlines, close to the interface of adhesive and adherent, where the kissing bond could occur, any small change in the interface would affect the EMI response of the sensor. The EMI behavior of the embedded sensor under static loading was studied. The single lap joints with sensors embedded inside the bondline were subjected to tensile tests with incremental load up to failure. The impedance was recorded under zero load condition before a higher load was exerted on the sample. A total of 16 samples were tested, while across all the tested samples a similar behavior was observed, i.e. the impedance of the sensor is kept constant until a certain load level, after which, the impedance changes dramatically from the pristine state. The root mean square deviation was defined as the damage index to quantify the change of impedance.

A finite element model was also developed to investigate the impedance behavior of the embedded piezo sensor. In order to simulate the behavior of kissing bond, the stiffness of the interface elements of the adhesive was degraded. The degradation of this 10 um thick element would not affect the global stiffness of the lap joint. However, it would affect the impedance behavior of the embedded sensors significantly. Preliminary simulation results matched with the experimental result qualitatively and similar trend of the decrease of resonant frequency was seen when the sample was prone to failure.

Both the experimental and simulation results indicate that the embedded piezoelectric sensor is sensitive enough to pick up the change of stiffness of the interface between the adhesive and adherents. In addition, due to the nature of the impedance based method, the change of stiffness of the cohesive region (such as the change due to disbond) would affect the impedance of the sensor more dramatically.

Future work will include the study of the effect of the sensors' locations in bondlines to improve the detectability; to validate the impedance-based algorithms under dynamic and fatigue loading; to investigate the temperature effects as the stiffness of the adhesive is sensitive to the ambient temperature; and the development of piezoelectric sensors with smaller dimension so that much less parasitic effect would be introduced when the sensor was embedded in the bondlines. An innovative piezoelectric ceramic sensor is being developed at Stanford University via screen-printed techniques. The screen-printed electric ceramic piezo-sensors can provide the needed EMI performance for the impedance-based algorithms for bondline integrity monitoring and meet the thickness requirements (typically 20~30 um) for bondlines application.

ACKNOWLEDGEMENT

This research was supported by the Boeing Company under the contract 9010406 and Air Force Office of Scientific Research (AFOSR) under the contract FA9550-13-1-0139. This work is also partially support from Multidisciplinary University Research Initiative (MURI) project under the contract FA9550-09-1-0677.

REFERENCES

1. Achenbach JD, Parikh OK. Ultrasonic analysis of nonlinear response and strength of adhesive bonds. *J. Adhes. Sci*. 1991 Jan 1;5(8):601-18.
2. Baltazar A, Rokhlin SI, Pecorari C. On the relationship between ultrasonic and micromechanical properties of contacting rough surfaces. *J. Mech. Phys. Solids*. 2002 Jul 31;50(7):1397-416
3. Baltazar A, Wang L, Xie B, Rokhlin SI. Inverse ultrasonic determination of imperfect interfaces and bulk properties of a layer between two solids. *J. Acoust. Soc. Am.* 2003 Sep;114(3):1424-34.
4. Adams RD, Drinkwater BW. Non–destructive testing of adhesively–bonded joints. *Int. J. Mater. Prod. Technol.* 1999 Jan 1;14(5-6):385-98.
5. Munns IJ, Georgiou GA. Non-destructive testing methods for adhesively bonded joint inspection: a review. *Insight*. 1995;37(12):941-52.
6. Brotherhood CJ, Drinkwater BW, Dixon S. The detectability of kissing bonds in adhesive joints using ultrasonic techniques. *Ultrasonics*. 2003 Sep 30;41(7):521-9.
7. Ehehart B, Valeskes B, Muller CE, et al. Methods for the Quality Assessment of Adhesive Bonded CFRP Structures -A Resumé. In: *2nd International Symposium on NDT*, Aerospace 2010, We.5.B.2
8. Kundu T, Maji A, Ghosh T, et al. Detection of kissing bonds by Lamb waves. *Ultrasonics*. 1998 Jan 1;35(8):573-80.
9. Nagy PB. Ultrasonic classification of imperfect interfaces. *J. Nondestr. Eval.* 1992 Dec 1;11(3-4):127-39.
10. Baltazar A, Rokhlin SI, Pecorari C. On the relationship between ultrasonic and micromechanical properties of contacting rough surfaces. *J. Mech. Phys. Solids.* 2002 Jul 31;50(7):1397-416.
11. Ren B, Lissenden CJ. Ultrasonic guided wave inspection of adhesive bonds between composite laminates. *Int. J. Adhes. Adhes.* 2013 Sep 30;45:59-68.
12. Lanza di Scalea F, Rizzo P, Marzani A. Propagation of ultrasonic guided waves in lap-shear adhesive joints: case of incident A 0 Lamb wave. *J. Acoust. Soc. Am*. 2004 Jan;115(1):146-56.
13. Jiao D, Rose JL. An ultrasonic interface layer model for bond evaluation. *J. Adhes. Sci. Technol.* 1991 Jan 1;5(8):631-46.
14. Light GM, Kwun H. Nondestructive evaluation of adhesive bond quality: state of the art review. *NTIAC* 1989 Jun.
15. Maeva E, Severina I, Bondarenko S, Chapman G, et al. Acoustical methods for the investigation of adhesively bonded structures: A review. *Can. J. Phys.*2004 Dec 1;82(12):981-1025.
16. Margetan FJ, Thompson RB, Gray TA. Interfacial spring model for ultrasonic interactions with imperfect interfaces: theory of oblique incidence and application to diffusion-bonded butt joints. *J. Nondestr. Eval.* 1988 Dec 1;7(3-4):131-52.
17. Rokhlin SI, Wang L, Xie B, et al. Modulated angle beam ultrasonic spectroscopy for evaluation of imperfect interfaces and adhesive bonds. *Ultrasonics*. 2004 Apr 30;42(1):1037-47.
18. Rokhlin SI, Xie B, Baltazar A. Quantitative ultrasonic characterization of environmental

degradation of adhesive bonds. *J. Adhes. Sci. Technol.* 2004 Jan 1;18(3):327-59.
19. Tang Z, Cheng A, Achenbach JD. An ultrasonic technique to detect nonlinear behavior related to degradation of adhesive bonds. *QNDE* 1998 (pp. 1347-1354). Springer US.
20. Wang N, Lobkis OI, Rokhlin SI, et al. "Ultrasonic Characterization of Interfaces in Composite Bonds." *AIP Conf. Proc.* 1335, 1079 (2011)
21. Ihn JB, Chang FK. Built-in Diagnostics for Monitoring Crack Growth in Aircraft Structures. In: *International Workshop on Structural Health Monitoring*. Stanford, CA, Sept 2001 pp. 284-295, Stanford: IWSHM
22. Ihn JB, Chang FK. Hot Spot Monitoring for Aircraft Structures. *Smart Mater. Struct.* 2004
23. Ihn JB, Chang FK. Detection and monitoring of hidden fatigue crack growth using a built-in piezoelectric sensor/actuator network: I. Diagnostics. *Smart Mater. Struct.* 2004 May 7;13(3):609-620.
24. Park G, Inman DJ. Impedance-based structural health monitoring. In: Inman DJ. et al (eds) *Damage prognosis for aerospace, civil and mechanical systems*. 2005 Dec 13:275-92.
25. Sun FP, Chaudhry Z, Liang C, et al. Truss structure integrity identification using PZT sensor-actuator. *J. Intell. Mater. Syst. Struct.* 1995 Jan;6(1):134-9.
26. Zagrai AN, Giurgiutiu V. Electro-mechanical impedance method for crack detection in thin plates. *J. Intell. Mater. Syst. Struct*. 2001 Oct 1;12(10):709-18.
27. Gulizzi V, Rizzo P, Milazzo A. On the Repeatability of Electromechanical Impedance for Monitoring of Bonded Joints. *AIAA Journal*. 2015 Oct 1;53(11):3479-83.
28. Annamdas VG, Soh CK. Application of electromechanical impedance technique for engineering structures: review and future issues. *J. Intell. Mater. Syst. Struct.* 2010 Jan 1;21(1):41-59.
29. Park G, Inman DJ. Structural health monitoring using piezoelectric impedance measurements. *Philos. Trans. A Math. Phys. Eng. Sci.* 2007 Feb 15;365(1851):373-92.
30. Roth W, Giurgiutiu V. Structural health monitoring of an adhesive disbond through electromechanical impedance spectroscopy. *Int. J. Adhes. Adhes.* 2017 Mar 31;73:109-17.
31. Na S, Tawie R, Lee HK. Electromechanical impedance method of fiber-reinforced plastic adhesive joints in corrosive environment using a reusable piezoelectric device. *J. Intell. Mater. Syst. Struct.* 2012 May;23(7):737-47.
32. Dugnani R, Zhuang Y, Kopsaftopoulos F, Chang FK. Adhesive bond-line degradation detection via a cross-correlation electromechanical impedance-based approach. *Struct. Health Monit.* 2016 Nov 1;15(6):650-67.
33. Zhuang Y, Kopsaftopoulos F, Chang FK. Bondline integrity monitoring of adhesively bonded structures via an electromechanical impedance based approach. In: *International Workshop on Structural Health Monitoring*. Stanford, CA, 2015 Sep 2.
34. Zhuang Y, Li YH, Kopsaftopoulos F, Chang FK. A self-diagnostic adhesive for monitoring bonded joints in aerospace structures, In *SPIE Smart Structures and Materials+ Nondestructive Evaluation and Health Monitoring* (pp. 98030I-98030I). International Society for Optics and Photonics, 2016.
35. Roy S, Lonkar K, Janapati V, Chang FK. A novel physics-based temperature compensation model for structural health monitoring using ultrasonic guided waves. *Struct. Health Monit.* 2014 Mar 19;13(3):321-342.